Primary Disease Gradients of Wheat Stripe Rust in Large Field Plots

Kathryn E. Sackett and Christopher C. Mundt

Botany and Plant Pathology Department, 2082 Cordley Hall, Oregon State University, Corvallis 97331.
Accepted for publication 30 April 2005.

ABSTRACT

Sackett, K. E., and Mundt, C. C. 2005. Primary disease gradients of wheat stripe rust in large field plots. Phytopathology 95:983-991.

Field data on disease gradients are essential for understanding the spread of plant diseases. In particular, dispersal far from an inoculum source can drive the behavior of an expanding focal epidemic. In this study, primary disease gradients of wheat stripe rust, caused by the aerially dispersed fungal pathogen *Puccinia striiformis*, were measured in Madras and Hermiston, OR, in the spring of 2002 and 2003. Plots were 6.1 m wide by 128 to 171 m long, and inoculated with urediniospores in an area of 1.52 by 1.52 m. Gradients were measured as far as 79.2 m downwind and 12.2 m upwind of the focus. Four gradient models—the power law, the modified power law, the exponential model, and the Lambert's general model—were fit to the data. Five of eight gradients were better fit by the power law, modified power law, and Lambert model than by the exponential, revealing the non-exponentially bound nature of the gradient tails. The other three data sets, which comprised fewer data points, were fit equally well by all the models. By truncating the largest data sets (maximum distances 79.2, 48.8, and 30.5 m) to within 30.5, 18.3, and 6.1 m of the focus, it was shown how the relative suitability of dispersal models can be obscured when data are available only at a short distance from the focus. The truncated data sets were also used to examine the danger associated with extrapolating gradients to distances beyond available data. The power law and modified power law predicted dispersal at large distances well relative to the Lambert and exponential models, which consistently and sometimes severely underestimated dispersal at large distances.

Additional keywords: multiple infection transformation, *Triticum aestivum*.

Dispersal is key to the development of plant disease epidemics, as it allows disease to spread in space, as well as in time. Studies of plant pathogen dispersal have been used to identify sources of inoculum (32) and dispersal mechanisms (5), to assess the importance of interplot interference in resistance and pesticide trials (26), and to attempt to predict the spatiotemporal behavior of plant disease epidemics over many pathogen generations (13).

Dispersal gradients of wind-dispersed pathogens such as rusts and powdery mildews are typically very steep, with most propagules traveling only a short distance from the source (16). However, the relatively few propagules traveling far from the source are crucial to disease spread. Simulations and analytic studies (7,13,23,27,28) indicate that the shape of the tails of dispersal gradients determine whether an epidemic will expand as a traveling wave (i.e., at a constant rate) or as a dispersive wave (i.e., with an epidemic velocity that increases over time). According to these studies, dispersal gradients with exponentially bound tails give rise to traveling waves, while those with non-exponentially bound tails yield dispersive-wave epidemics.

Although dispersal far from a source may drive the behavior of an epidemic, acquiring field data to characterize gradient tails adequately can be difficult. The requirement for a large amount of land can be prohibitive, and strong sources must be used to provide measurable disease levels at long distances. Contamination by outside inoculum can also confound attempts to measure dispersal in the tail of a gradient, where disease levels are low. For the current study, we measured primary disease gradients of wheat stripe rust (caused by *Puccinia striiformis*) in a large-scale experiment in order to determine the shape of the dispersal gradient. The experiment was conducted at two locations chosen to avoid outside inoculum, and was designed to minimize interplot interference.

Corresponding author: K. E. Sackett
E-mail address: sackettk@science.oregonstate.edu

DOI: 10.1094/PHYTO-95-0983

MATERIALS AND METHODS

Field plots. Field experiments were conducted at Hermiston and Madras, OR, during the spring of 2002 and 2003 as part of a larger study on the effect of cultivar mixtures on epidemic velocity (4). Both sites experience prevailing winds from the west, Hermiston having both stronger winds and stronger directionality than Madras. The growing season is earlier, warmer, and drier at the Hermiston site, in the Columbia Basin of eastern Oregon, than at Madras, which is located just east of the Cascade Mountains in central Oregon. Weather stations recorded temperature, wind, precipitation, humidity, and other variables at both sites. No wheat cultivars susceptible to *P. striiformis* were commonly grown in either area at the time this study was conducted, and risk of contamination of field plots by indigenous populations of the pathogen was considered low.

Winter wheat cv. Jacmar was planted in the fall of each year in three replicate plots measuring 6.1 m wide by 128 to 171 m long, oriented parallel to the dominant wind direction (Fig. 1). The plots of 'Jacmar', which is susceptible to *P. striiformis*, were separated from one another and from mixed-cultivar plots (not involved in this part of the study) by buffer zones planted to resistant winter wheat cv. Stephens (16.8 m wide in Hermiston, 30.5 m wide in Madras). In Hermiston, the plots were placed inside one quarter of an irrigation circle, so plot lengths varied. Planting density was 323 seeds per m^2. Each 6.1-m-wide plot consisted of four passes of a six-row seed drill with a 1.52-m wheel base. Row spacing within each pass was 0.20 m. Standard commercial cultural practices for each location were applied, in-

cluding regular irrigation starting in early spring (once per week in Madras, three to five times per week in Hermiston).

An area (1.52 by 1.52 m) of each plot was inoculated with *P. striiformis* race CDL 5 (CDL = USDA-ARS Cereal Disease Laboratory, Pullman, WA) in the spring of each year, when plants were at growth stage 4 to 5 on the Feekes scale (3). This focus was placed in the center of the plot widthwise, and was shifted upwind of the center lengthwise (Fig. 1). The inoculations were accomplished by first spraying the wheat plants with water and then dusting them with a 1:10 mixture of urediniospores and talc powder under a tent of plastic sheeting the same size as the inoculated square. Freshly collected spores were used whenever possible; frozen spores were used to augment the inoculum when the supply of fresh spores was insufficient. Since frozen spores are known to be less viable than fresh, frozen spores replaced fresh spores in a ratio of 3:1. Within each experiment, foci received equal amounts of inoculum. Among experiments, inoculum varied from 0.25 to 0.46 g of urediniospores per focus. After inoculation, plants were covered overnight with a plastic sheet, preventing spread of spores beyond the intended inoculation area, as well as ensuring an environment moist enough for spore germination and infection.

Disease assessments. For the larger study (4), weekly assessments of disease severity were made beginning at the appearance of sporulating lesions through the end of the growing season. In order to characterize the primary disease gradient for the current study, an intensive disease assessment was conducted 7 to 9 weeks after inoculation. For each of the four experiments, this date was chosen to be shortly after the appearance of the second generation of the pathogen, and before the appearance of the third generation. The timing was based on observations of new stripe rust lesions outside the inoculated focus. The estimated number of latent periods between inoculation and gradient assessment, based on degree-hour calculations (29), was 2.42, 2.90, 2.92, and 2.57 in Hermiston 2002 and 2003 and Madras 2002 and 2003, respectively (average latent periods 18.0 to 24.6 days). Assessments were made at markers in the focus, at 0.9, 1.5, 2.1, 3.0, 4.6, 6.1, 9.1, and 12.2 m from the center of the focus, and at every 6.1 m thereafter in both the upwind and downwind directions. The outermost marker in each direction was 6.1 m or more from the edge of the plot to avoid the eddying effects that sometimes occur there.

At each marker, two 0.3-m sections of plants were assessed, one in the second row north of the center aisle (where the planter tires ran during planting), and one in the second row south of the aisle. The centers of these rows were 0.9 m apart. In each section, the total number of lesions on a designated leaf of each tiller was counted, as was the number of tillers. The designated leaf was the F-3 leaf in Hermiston both years, the flag leaf (F) in Madras 2002, and the F-2 leaf in Madras 2003. In each case, the leaf was chosen to maximize the amount and accuracy of information gathered. Leaves higher on the plant had fewer lesions, and the counts decreased to zero not far from the focus. Lower leaves had more lesions, which coalesced at high severities, making individual lesions difficult to discern and count. In 2002 at both locations, the level of disease near the focus was too high to count individual lesions on the designated leaf. At these markers only, severity (percent leaf area covered by lesions) was assessed and later converted to an approximate lesion count by estimating the maximum possible number of lesions per leaf. This procedure was followed at five markers (0 to 3.0 m downwind) in Hermiston and three markers (0 to 1.5 m downwind) in Madras. All three replicate plots were assessed in each experiment, except at Hermiston in 2002, where the shortest of the three plots had planting irregularities that prevented accurate assessment. The entire assessment for each of the four experiments took place in either a single day or two consecutive days. Each plot was completed in a single day.

Data analysis and model fitting. Data were expressed as the mean number of lesions per leaf for each sampling location. These raw lesion count data represent the primary disease gradient (except in the focus, where two generations of the pathogen were superimposed). To characterize the dispersal gradient, an adjustment was made for multiple infections. Assuming a finite number of infection sites on a leaf's surface, and assuming that, on the scale of a leaf, established infections reduce the likelihood of new infection in proportion to the number of sites they occupy, the number of "effective spores" required to achieve y lesions of N total possible lesions on that leaf is $N\ln[N/(N - y)]$ (15). The term "effective spores" is defined as those spores that, in the ab-

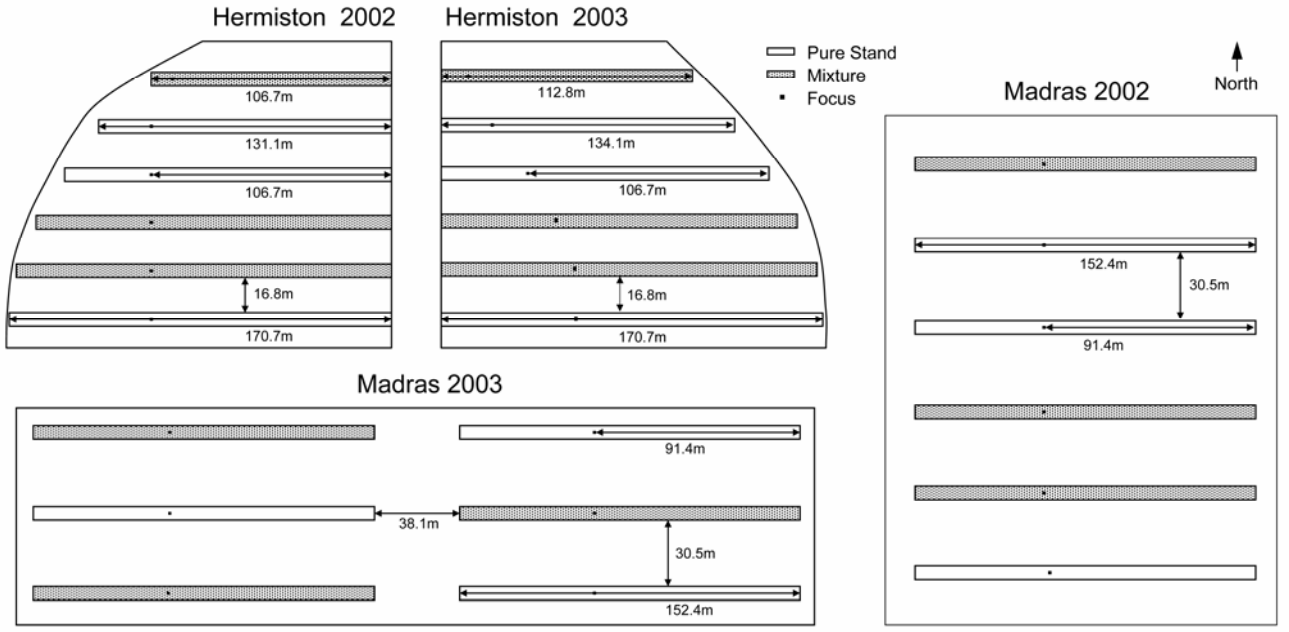

Fig. 1. Plot layouts for wheat stripe rust field experiments in Hermiston and Madras, OR, in 2002 and 2003. Pure-stand plots were planted to susceptible 'Jacmar' and mixtures contained both 'Jacmar' and resistant 'Stephens.' Gradient data presented in this paper are from pure-stand plots. Plots were 6.1 m wide; inoculated foci were 1.52 × 1.52 m. Prevailing winds for both sites are generally from the west.

sence of prior infection, would succeed in causing a lesion. Following Minogue's advice (22), the transformation was applied to severity values >10%. None of the data points originally collected as lesion counts corresponded to severities high enough to necessitate the transformation.

In the focus, quantifying the second generation of the pathogen was complicated by the presence of the first generation. (Here, the convention is that the "zeroth" generation consists of the spores used in the inoculation; the first generation consists of the initial lesions in the focus; and the second generation consists of lesions caused by the spores of the first generation.) The principles of the multiple infection transformation were applied in order to estimate dispersal of spores to the focus from infected plants within the focus. As an illustration of the calculation, assume the severity of the first generation of lesions on a leaf to be 34%. If the number of possible infection sites per leaf is 100, then 34 sites are filled. The multiple infection transformation predicts that 42 effective spores would be necessary to achieve that severity. Assume also that after the second generation appears, the severity is 95%. According to the transformation, a total of 300 effective spores would be required. The difference (300 – 42 = 258) is the number of effective spores needed to increase the severity on that leaf from 34 to 95%, and this figure may be used to quantify the second generation in the focus. Similar calculations were made for the focus in each of the four experiments using the severity at the time when the primary disease gradient data were gathered (first plus second generation) and the severity 2 weeks prior (first generation).

The number of lesions per leaf at each distance upwind and downwind of the focus, transformed as described above, was then averaged over replicates. Lesion counts vary from focus to gradient tail by several orders of magnitude, which means that fitting models based on untransformed counts would result in the few large values near the focus overly influencing the outcome. Conversely, the small values in the tails would contribute so little to the sum of squares of the residuals that they would become almost irrelevant to the estimation of model parameters. This is undesirable, particularly in light of the demonstrated importance of the shape of the tail of the gradient. Transformation using the natural logarithm allows small but biologically significant changes in lesion density in the tail of the gradient to have an appropriate influence on the fit of the models. All lesion count data were therefore $\log_e$-transformed prior to analysis.

Data points with mean zero present a complication when using the log transformation, since the logarithm is undefined at zero. One approach is to add some arbitrarily small value to zeroes before transformation. This method can introduce bias, however, since those small values may become quite influential in the log-transformed space. Instead, we chose to simply exclude the zeroes from the analyses. Moving outward from the focus, all nonzero points beyond the first zero were also excluded. Including nonzero data points while excluding the zeroes would artificially inflate the apparent lesion density in these regions.

In order to characterize the shapes of the primary disease gradients, several models with different tail shapes were fit to the data: the exponential (18),

$$y = a\exp(-bx) \quad (1)$$

which describes a curve with exponentially bound tails; the (inverse) power law (16),

$$y = ax^{-b} \quad (2)$$

which has non-exponentially bound tails, but has the disadvantage of not being defined at the source ($x = 0$); the modified power law (25),

$$y = a(x + c)^{-b} \quad (3)$$

which is similar in shape to the power law, but has a finite value at the source; and the general model proposed by Lambert et al. (19),

$$y = a\exp(-bx^n) \quad (4)$$

which can take on a variety of shapes, from a power law (as n approaches 0), to an exponential ($n = 1$), to a Gaussian (normal) curve ($n = 2$). In each equation above, y is the amount of disease at a distance x from the source, a is proportional to the strength of the source, and b is a measure of the steepness of the gradient. In the modified power law, c is an offset parameter greater than zero and is expressed in units of distance.

Log_e-transformed versions of the models were fit to the logged lesion count data. The transformed models are as follows:

Exponential: $\ln y = \ln a - bx$ (5)

Power law: $\ln y = \ln a - b\ln x$ (6)

Modified power law: $\ln y = \ln a - b\ln(x + c)$ (7)

Lambert: $\ln y = \ln a - bx^n$ (8)

Models were fit to each of the eight data sets (two directions × two locations × 2 years) using nonlinear least squares regression (nls function of S-PLUS, Insightful Corp., Seattle, WA). (Equations 5 and 6 could also be fit using simple linear regression, which would result in identical parameter estimates.) The focus ($x = 0$) was excluded when fitting the power law, since the model is undefined there. In the case of the modified power law, two different regressions were carried out for each data set. In the first, all three parameters were estimated concurrently. In the second, the offset parameter, c, was fixed at the half-width of the inoculated focus (0.76 m) before estimating the other two parameters, because c has been postulated to approximate the radius of the source (2, 24,25). To evaluate the relative abilities of the models to fit each data set, coefficients of determination (R^2) were calculated based on the log-transformed data, and residual plots were examined.

The three largest data sets (downwind gradients for Hermiston 2002, Madras 2002, and Madras 2003, with maximum distances 79.2, 48.8, and 30.5 m, respectively) were used to investigate the ability of the gradient models to predict dispersal, given data with a limited distance range. The data sets were truncated to within 30.5, 18.3, and 6.1 m of the focus, and regressions were performed to fit the gradients models as described above. Fitted curves derived from the truncated data sets were compared with the full data sets to see how well extrapolations based on those curves described dispersal in the tails of the gradients. R^2 values were calculated from the reduced data sets.

Ferrandino (8) proposed a formal statistical test to determine whether a data set is significantly better fit by the power law or the exponential. This F test was performed on all eight data sets, as well as the truncated ones derived from the three largest data sets. Since the power law is not defined at $x = 0$, observations in the focus were not included for this test.

RESULTS

In both locations and both years, primary disease gradients were steeper upwind than downwind, which is evident from estimates of b for the power law and exponential models, as well as for the modified power law with c fixed (Table 1). This result is typical for wind-dispersed pathogens in locations having a prevailing wind direction (10,11). (Correlation among parameter estimates for the three-parameter modified power law and Lambert model means that b estimates from these models should not be used directly to evaluate gradient steepness.) During dispersal of the first generation of spores out of the inoculated focus, the Hermiston site experienced strong winds from the west in both years. Winds were not as strong and not as consistently from the west at the Madras site: during the dispersal period in 2002, winds were

mostly from the north and northwest; southwest winds dominated in 2003 (Fig. 2).

Stand density, which may influence dispersal of spores (11), differed among the two sites and years. Although seeding rates were the same, plants produced more tillers in Madras (130 and 173 tillers per m in 2002 and 2003, respectively) than in Hermiston (113 and 69 tillers per m in 2002 and 2003, respectively).

Although field plots were of similar size in both years and both locations, the distance over which nonzero lesion counts were observed varied (Fig. 3). The largest data set, which extended 79.2 m from the center of the focus, was from Hermiston 2002, where the initial inoculation was highly successful. First-generation severity in the focus was 22.7% compared with 6.2% in Madras 2002, 0.0067% in Hermiston 2003, and 5.5% in Madras 2003. Weather conditions were especially conducive to infection by *P. striiformis* in Hermiston 2002 immediately after inoculation, as indicated by dew point temperatures. Those plots also received the largest amount of inoculum, 0.46 g, although that amount included the largest portion of frozen spores, 0.32 g, which were assumed to be less viable than fresh spores. The production of large amounts of spores in the inoculated focus was crucial for producing detectable disease levels far away from the source. In contrast, Hermiston had little or no dew following inoculation in 2003, and relatively weak initial establishment of disease. Inoculum level was also the lowest then, with 0.25 g fresh spores per plot. As a result, Hermiston 2003 had the smallest downwind data set, extending only 4.6 m from the center of the focus. Upwind data sets also tended to be small (3.0 to 12.2 m) since fewer spores travel upwind than downwind.

For each of the eight data sets, there were one or two nonzero observations beyond the first zero. Eight of eleven of these were single lesions found in only one of the replicates, which reflects the stochastic nature of the dispersal process at very low inoculum levels. Beyond the farthest nonzero observation in each data set, three to five additional zero observations were made (extending 12.2 to 30.5 m beyond the last lesion found), except in Hermiston 2002, where two lesions were found at the 97.5-m marker, the last marker before the end of the plot. This mixture of zero and nonzero observations in the tail is consistent with a lesion density less than one lesion per sampling location.

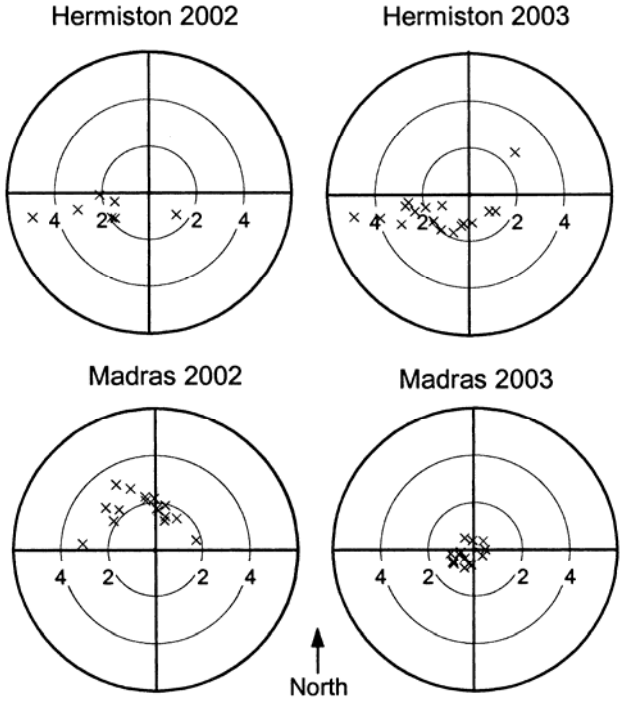

Fig. 2. Daily average wind speed (meters/second) and direction during dispersal of the first generation of *Puccinia striiformis* spores from the inoculated focus during four field experiments. Dates are between one latent period after inoculation and one latent period before primary disease gradient assessment, based on degree-hour calculations (29).

TABLE 1. Parameter estimates and coefficients of determination (R^2) derived from fitting four models to primary disease gradient data of wheat stripe rust from two locations (Hermiston and Madras, OR) in 2 years[a]

	Downwind				Upwind			
Model	*a*	*b*	*c* or *n*	R^2	*a*	*b*	*c* or *n*	R^2
Hermiston 2002								
Exponential	18.59	0.106	…	0.776	10.91	0.658	…	0.728
Power law (focus excluded)	184.9	2.07	…	0.990	4.907	2.28	…	0.969
Modified power law	431.8	2.29	0.848	0.987	6.912	2.42	0.180	0.988
Modified power law (*c* fixed)	380.4	2.25	0.762	0.987	55.46	3.41	0.762	0.954
Lambert	895.9	2.85	0.312	0.962	452.0	4.84	0.310	0.987
Hermiston 2003								
Exponential	4.979	1.005	…	0.966	5.61	1.048	…	0.946
Power law (focus excluded)	1.653	1.94	…	0.944	3.024	2.86	…	0.989
Modified power law	255.0	4.26	2.28	0.991	12,685	6.16	3.183	0.979
Modified power law (*c* fixed)	5.052	2.40	0.762	0.976	7.548	3.00	0.762	0.943
Lambert	7.848	1.66	0.692	0.996	9.797	1.74	0.743	0.968
Madras 2002								
Exponential	2.372	0.149	…	0.552	13.11	1.011	…	0.846
Power law (focus excluded)	14.20	2.09	…	0.876	6.824	3.27	…	0.987
Modified power law	17.25	2.12	0.332	0.896	66.02	4.20	0.858	0.989
Modified power law (*c* fixed)	40.50	2.39	0.762	0.885	45.87	4.03	0.762	0.988
Lambert	227.9	3.92	0.265	0.841	133.9	3.64	0.483	0.974
Madras 2003								
Exponential	1.805	0.245	…	0.854	7.375	3.024	…	0.905
Power law (focus excluded)	5.804	2.11	…	0.953	0.596	5.84	…	0.918
Modified power law	112.6	3.02	2.34	0.964	2.56E+16	20.9	5.468	0.912
Modified power law (*c* fixed)	10.16	2.24	0.762	0.945	3.499	5.56	0.762	0.870
Lambert	10.30	1.59	0.490	0.947	8.626	3.31	0.923	0.906

[a] *a*, *b*, *c*, and *n* are parameters of the models fit to the gradient data. The models are as follows: exponential, $y = a\exp(-bx)$; power law, $y = ax^{-b}$; modified power law, $y = a(x + c)^{-b}$; and Lambert, $y = a\exp(-bx^n)$; where *y* is the number of lesions per leaf at a distance *x* (in meters) from the center of the inoculated focus. *y* was transformed using the natural logarithm prior to analysis, and R^2 values are based on nonlinear regression with the transformed data (described in text). Where *c* of the modified power law was fixed, its value was the half-width of the inoculated focus (0.76 m).

Plots of log-transformed lesion counts versus distance (such as those in Fig. 3) indicated that the power law, modified power law, and Lambert model fit the dispersal data considerably better than the exponential did for the five largest data sets: Hermiston 2002 upwind and downwind, Madras 2002 upwind and downwind, and Madras 2003 downwind. Curvature in these plots implies a lack of fit to the exponential model, since it is linear in x when log-transformed. This conclusion was confirmed by the R^2 calculations (Table 1) and residual plots (Fig. 4). The other three data sets, each of which consisted of seven or fewer observations and extended no farther than 6.1 m from the focus, were equally well described by all of the models (Table 1, Fig. 3).

The three largest data sets (Hermiston 2002 downwind, and Madras 2002 and 2003 downwind), which had the most curvature in the log-linear plots, were also indicated by Ferrandino's F test (8) to be significantly better fit by the power law than the exponential ($P < 0.05$). This formal statistical test is a more stringent method of determining whether gradient tails are exponentially bound, compared with R^2 values or log-linear plots.

In the five cases where there was a difference in goodness of fit among the models, the exponential always underestimated values near the source and in the tail of the gradient (Figs. 3 and 4). For each data set, the shapes of the fitted curves were similar for the power law, modified power law, and modified power law with c fixed (data not shown). The R^2 values for these three models also tended to be about the same for a given data set, although it should be noted that the unmodified power law was fit to a reduced data set (focus excluded).

The Lambert model performed as well as the three versions of the power law in most cases, but showed slightly more bias in the

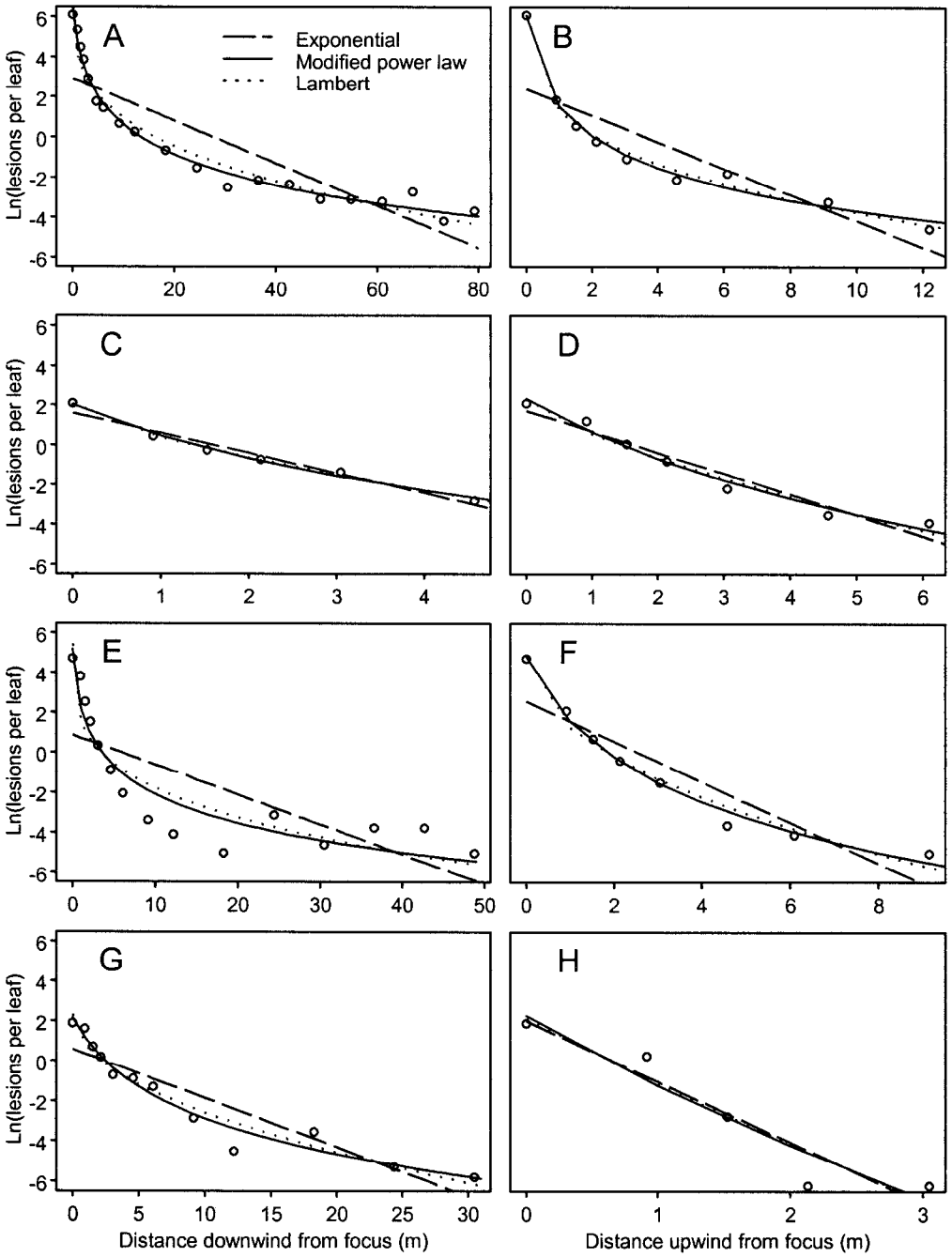

Fig. 3. Three models fit to primary disease gradients of wheat stripe rust from four field experiments. Data are from Hermiston, OR, 2002 (**A and B**) and 2003 (**C and D**) and Madras, OR, 2002 (**E and F**) and 2003 (**G and H**), either downwind (**A, C, E, and G**) or upwind (**B, D, F, and H**) of the inoculated focus. Open circles are means of two or three replicate plots.

residual plots in the two largest data sets (Hermiston and Madras 2002 downwind). The Hermiston 2002 downwind data set was the largest and shows the clearest differences among the models (Fig. 4). In all cases, the estimated value of the shape parameter of the Lambert model, n, was between 0 and 1, indicating a non-exponentially bound tail shape intermediate between the power law and the exponential.

Truncating the three largest data sets and then fitting the models to these reduced data sets revealed the consequences of not collecting data far enough from the source (Figs. 5 and 6). R^2 values for the different models tended to be closer together when less data were used in the regressions. In fact, if data had been available only to 6.1 m from the focus, all of the models would have appeared to fit the data equally well (R^2 values for three of the five models are shown in Fig. 5). This distance range is comparable to the range of many previous gradient studies. Limited range may also be the reason that no difference in the fit of the models was detected in three of the data sets, which extended to 3.0, 4.6, and 6.1 m from the focus (Madras 2003 upwind, and Hermiston 2003 upwind and downwind, respectively). Although the gradient shapes may have been similar to those of the larger data sets, low disease levels prevented detection at distances far enough from the focus to determine the relative suitability of the models.

It is also instructive to examine how well the models predict values in the tails of the gradients, given limited data. The three power law models best predicted dispersal for distances beyond those used in the regressions (Fig. 6). The unmodified, two-parameter power law fit the data well, regardless of the amount of data provided. A disadvantage of this model is that observations in the focus cannot be included. The modified power law with c fixed at the half-width of the focus did at least as well as the others in predicting dispersal far from the source, although it underestimated values near the source. When all three parameters of the modified power law were estimated concurrently, the model performed well. However, the 6.1-m truncation of the Hermiston 2002 and Madras 2002 data (Fig. 6) shows that the extra flexibility of allowing c to vary can lead to underestimation in the tails of the gradient.

The exponential model, which has already been shown to fit data in the current study poorly, underpredicted the tails of the gradients by an even greater amount when the data was truncated (Fig. 6). The fitted line became steeper as the amount of data used to fit the model was reduced (a phenomenon also noted by Aylor [1]). So, although the underestimation by the exponential of dispersal far from the source was more severe when less data was available, R^2 values based on the limited data sets would falsely imply that the model fit is comparable to the other models examined here (Figs. 5 and 6).

The Lambert model, which like the modified power law has the flexibility of three free parameters, also underestimated dispersal far from the source when the data set was truncated, although somewhat less than the exponential (Fig. 6).

Results from Ferrandino's F test (8) showed the difficulty in distinguishing between the fit of the power law and the exponential when limited data are available. They indicated no significant difference in the fit of the power law versus the exponential for any data set with a range <18.3 m ($P > 0.05$), including the artificially truncated ones. The F test indicated the superior fit of the power law over the exponential for the complete data set from Madras 2003 downwind (maximum distance 30.5 m), as well as the Hermiston and Madras 2002 downwind gradients even when

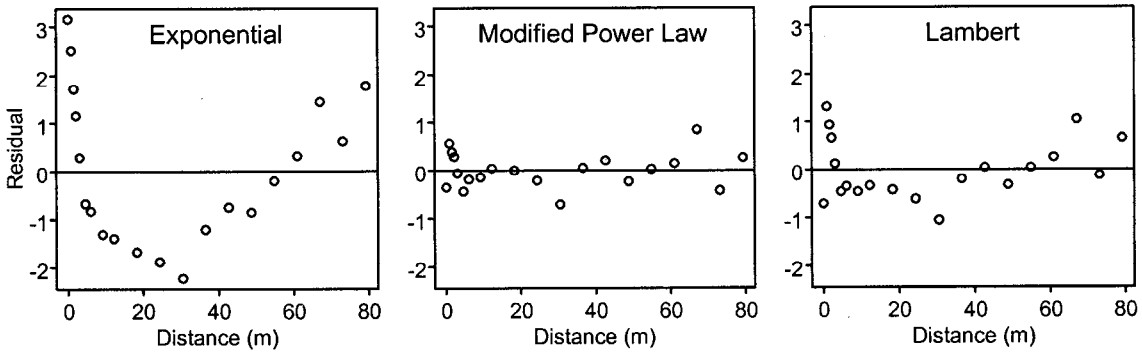

Fig. 4. Example of typical disease gradient residual plots: observed minus predicted values for ln(lesions per leaf) for three gradient models. Field data are from a wheat stripe rust epidemic in Hermiston, OR, in 2002. Data points represent the means of two replicate plots. Distances were measured downwind of the inoculated focus.

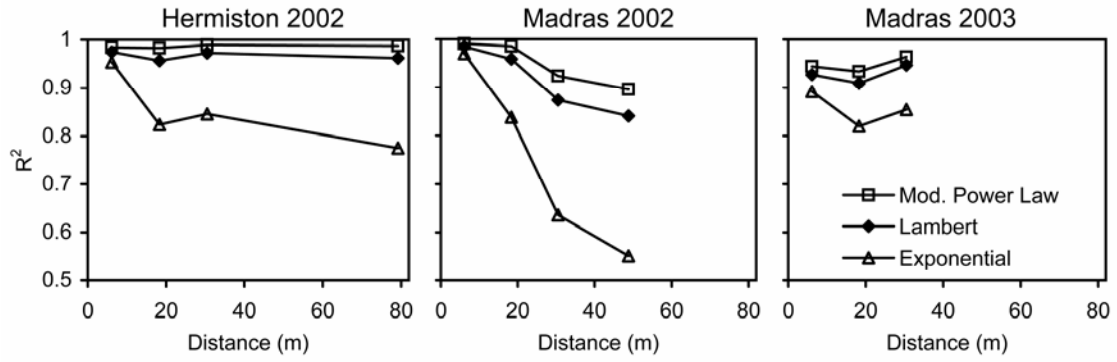

Fig. 5. Coefficients of determination (R^2) for fit of three models to complete or truncated disease gradients of wheat stripe rust. Models were fit to three complete downwind data sets (maximum distances 79.2, 48.8, and 30.5m for Hermiston 2002, Madras 2002, and Madras 2003, respectively), then to the same data sets truncated to 6.1, 18.3, and 30.5 m. Gradient data were transformed using the natural logarithm prior to analysis, and R^2 values are based on the transformed data. R^2 values were calculated using only the data points included in each regression.

these were truncated to 30.5 or 18.3 m ($P < 0.05$). Put another way, of the three gradients that Ferrandino's F test (8) indicated were significantly better fit by the power law, none revealed this characteristic within 6.1 m of the focus.

Because the Madras 2002 downwind gradient did not decline smoothly with distance after 18.3 m, none of the models were able to fit the data well over the entire distance range, regardless of whether the data were truncated. This flattening of the gradient tails after an initial smooth decrease was not observed in any other data set, and may have been caused by exchange of spores between plots. Winds during dispersal that year were predominantly from the north, not from the west as is usually the case in Madras (Fig. 2). Therefore, the east-west orientation of the plots was not ideal for preventing interplot interference. In the southernmost plot, which was separated from the other pure-stand plots by two mixture plots plus 91.5 m of resistant buffer plants (Fig. 1), no lesions were observed past 12.2 m downwind (assessments were made to 85.3 m). Mixture plots were also inoculated, but produced approximately 18% as many spores as pure-stand plots. The other two pure stands were adjacent to one another, and both showed the fat-tailed pattern, which was less marked in the northern plot. This is consistent with more inoculum arriving in the southern plot from the northern one than vice versa, due to the north winds. Wind patterns in the other three experiments were

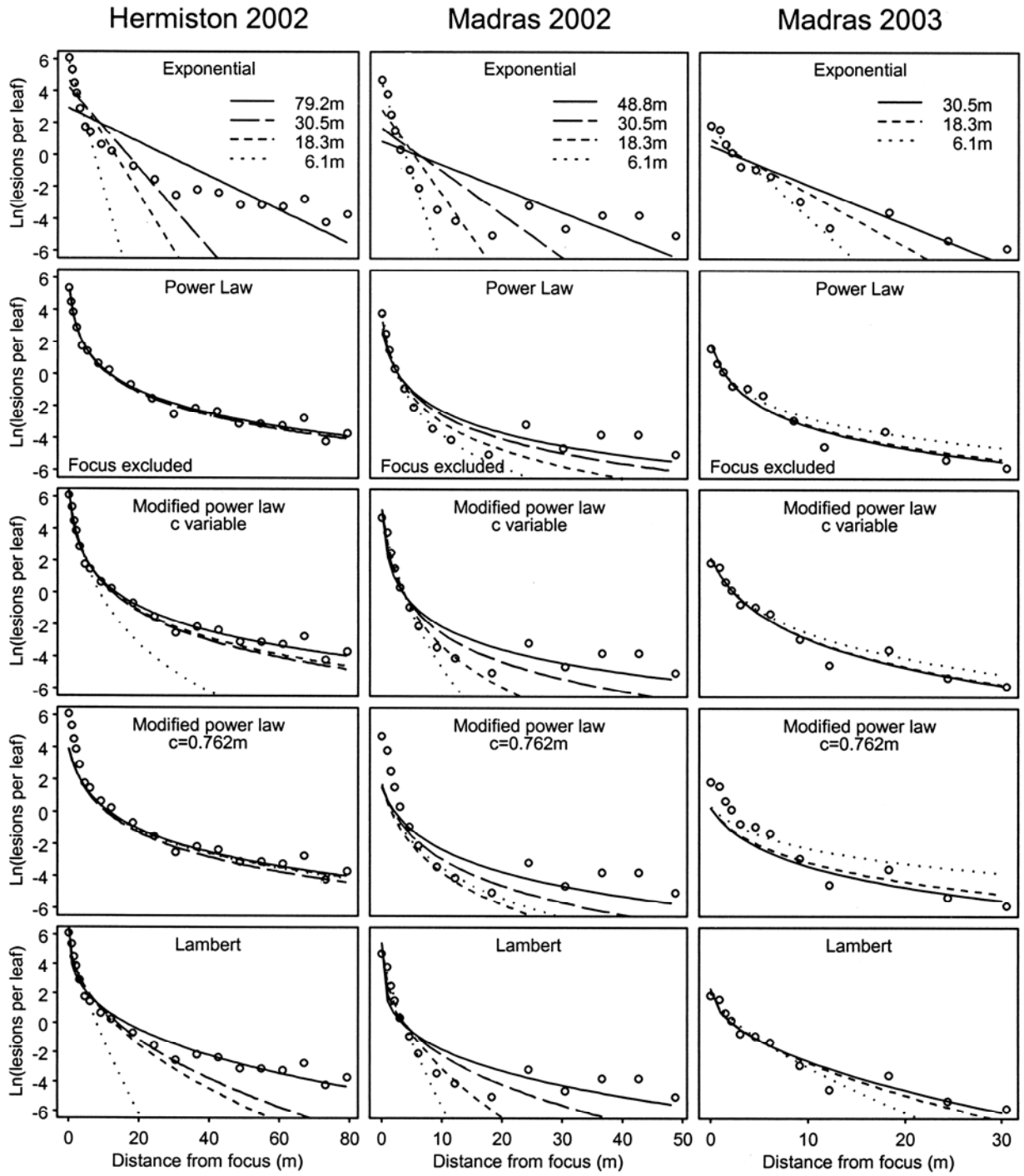

Fig. 6. Five gradient models fit to downwind disease gradients of wheat stripe rust from three field experiments. Models were fit either to all available data (solid lines) or truncated data (broken lines). Open circles are means of two or three replicate plots. Legends show the distance from the focus to the farthest data point used for model fitting. The focus (distance = 0) was excluded from power law calculations.

less likely to produce interplot interference. Wind was strong and almost always from the west in Hermiston both years (Fig. 2), so winds likely were blowing spores mainly along the length of the plots rather than between them. In Madras 2003, the winds were not as directional, but they were also weaker (Fig. 2), so the likelihood of interplot interference causing detectable disease was low. The plot arrangement was also different, with no two pure-stand plots being adjacent (Fig. 1), and there were no discernable differences in the gradients among the three plots.

DISCUSSION

Given the significance of gradient tails to plant disease spread, collecting dispersal data far from a source of inoculum is essential. Gradient studies typically measure dispersal to distances of less than 10 m (1,2,9,12–14,20,21,25). A few extended their observations to 10 to 30 m from the source (5,9,17,24), and de Luna et al. (6) used rotorod samplers to evaluate dispersal up to 50 m away. Many of these studies were also limited in the number of sampling locations (most had around seven). In this study, we were able to measure a primary disease gradient of wheat stripe rust to as far as 79.2 m, with as many as 20 sampling locations, yielding ample information to examine the nature of the gradient tails.

In the cases where we were able to find lesions far enough from the source to distinguish among the fit of different models, the gradients were clearly better fit by non-exponentially bound models (the power law, modified power law, and Lambert models) than by the exponential model. This characteristic has implications for the spread of wheat stripe rust over many pathogen generations, and indeed the epidemics that developed after measurement of these primary disease gradients expanded as dispersive waves (4), as predicted theoretically (7,13,23,27,28).

Dispersal data can be difficult to acquire far from the source. The first requirement, of course, is for sufficient space to make long-distance observations. Other factors also come into play. One is source strength. Since such a small fraction of propagules travel far from the source, a very large amount of inoculum must be produced in order to result in detectable disease in that region. The present study illustrates this point. The most successful inoculation and highest disease levels were in the Hermiston 2002 experiment, which yielded the most extensive gradient data. In comparison, the inoculation in Hermiston 2003 was not as successful, lower disease levels were observed, and lesion counts trailed off to zero after only 6.1 m.

Inoculum from outside experimental plots can also present a difficulty in gradient studies. Close to a source, where disease is relatively high, a low level of background contamination may have little effect. Farther from the source, however, disease caused by experimental and outside inoculum may be of the same order of magnitude, confounding assessment of the gradient tails. Since no wheat varieties susceptible to stripe rust were grown near Hermiston or Madras at the time of these experiments, the opportunity existed to measure disease gradients without this complication. Another complication in assessing disease gradients is that interplot interference may play a part when replicate plots are placed near one another. In this study, replicate plots were separated by wide buffer zones of stripe rust-resistant plants and laid out in the field parallel to the predominant wind direction to minimize interference. In the one instance (Madras 2002) when winds during the dispersal period were not from the expected direction, data suggested that the observed gradients may have been influenced by inoculum from other plots in the field. In the other three cases, this influence does not appear to be significant, however. Preliminary simulations (using EPIMUL; 27,31) based on worst-case estimates of cross-wind dispersal indicated that, although there may have been some exchange of inoculum between plots, the effect on the shape of the measured gradients was likely minimal (*unpublished data*). In simulations, exponential gradients superimposed on exponential gradients remained exponential; fat-tailed gradients also retained their shape in the presence of additional fat-tailed sources.

Another factor to consider in designing gradient experiments is that a sampling technique must be chosen that is capable of detecting very low levels of disease. Time and labor constraints may make this a limiting factor in some situations.

Since gradient data are often available only near the source of disease propagules, those constructing models of disease spread may be forced to make assumptions—explicit or implicit—regarding the behavior of gradients at distances beyond the available data. With the three largest data sets presented here, it was possible to address the question of whether, if less extensive data had been available, a simple gradient model would be capable of giving reasonable estimates of dispersal in the tails of the gradient. The exponential model, which fit none of the large data sets well, seemed to fit the gradients acceptably when data was included to only 6.1 m from the focus. However, with so little data, the underestimation of dispersal in the tails was quite severe. Using the exponential model to estimate dispersal when a fat-tailed distribution is more appropriate could lead to underestimation of interplot interference, and incorrect predictions of epidemic velocity.

Of the four remaining models, the two with only two free parameters—the power law and the modified power law with c fixed—predicted the shape of the tails of the gradients the best. The modified power law and the Lambert models each contain one additional parameter, which provides additional flexibility but apparently allows the models to be more easily "mislead" by limited data. This tendency was more pronounced for the Lambert model. When models were inaccurate in extrapolating beyond the available data, the error was almost always an underprediction. The modified power law with c fixed at the radius of the source may be a reasonable model when limited data are available, and may be preferred over the power law, since focus values can be included.

In conclusion, under some circumstances, it is possible to measure disease gradients well enough to characterize the nature of their tails. Data may need to be gathered at relatively large distances from the source of pathogen propagules, however, to make this determination. A variety of factors, including small plot size, low disease levels, and insufficiently sensitive sampling techniques, can hinder the collection of sufficient data. The length scale required to characterize gradient tail shapes likely differs depending on the pathosystem and environmental conditions such as wind speed. More information is needed about the shape of dispersal gradients to help resolve the question of whether, and under what circumstances, traveling or dispersive epidemic waves exist (30). They are hypothesized to be associated with exponentially bound and non-exponentially bound dispersal gradients, respectively (7,13,23,27,28). In this study, gradients of wheat stripe rust were fit better by non-exponentially bound functions (power law, modified power law, or Lambert) whenever there was a difference in fit among models. And indeed, all of the epidemics that developed following the gradient measurements presented in this paper spread as dispersive waves (4).

ACKNOWLEDGMENTS

We thank the staff members at both the Hermiston and Madras field stations, who were instrumental to the success of this project.

LITERATURE CITED

1. Aylor, D. E. 1987. Deposition gradients of urediniospores of *Puccinia recondita* near a source. Phytopathology 77:1442-1448.
2. Aylor, D. E., and Ferrandino, F. J. 1990. Initial spread of bean rust close to an inoculated bean leaf. Phytopathology 80:1469-1476.

3. Campbell, C. L., and Madden, L. V. 1990. Introduction to Plant Disease Epidemiology. John Wiley & Sons, New York.
4. Cowger, C., Wallace, L. D., and Mundt, C. C. 2005. Velocity of spread of wheat stripe rust epidemics. Phytopathology 95:972-982.
5. Cox, K. D., and Scherm, H. 2001. Gradients of primary and secondary infection by *Monilinia vaccinii-corymbosi* from point sources of ascospores and conidia. Plant Dis. 85:955-959.
6. de Luna, L., Bujold, I., Carisse, O., and Paulitz, T. C. 2002. Ascospore gradients of *Gibberella zeae* from overwintered inoculum in wheat fields. Can. J. Plant Pathol. 24:457-464.
7. Ferrandino, F. J. 1993. Dispersive epidemic waves: I. Focus expansion within a linear planting. Phytopathology 83:795-802.
8. Ferrandino, F. J. 1996. Length scale of disease spread: Fact or artifact of experimental geometry. Phytopathology 86:806-811.
9. Ferrandino, F. J., and Aylor, D. E. 1987. Relative abundance and deposition gradients of clusters of urediniospores of *Uromyces phaseoli*. Phytopathology 77:107-111.
10. Fitt, B. D. L., Gregory, P. H., Todd, A. D., McCartney, H. A., and Macdonald, O. C. 1987. Spore dispersal and plant disease gradients; A comparison between two empirical models. J. Phytopathol. 118:227-242.
11. Fitt, B. D. L., and McCartney, H. A. 1986. Spore dispersal in relation to epidemic models. Pages 311-345 in: Plant Disease Epidemiology, Vol. 1. K. J. Leonard and W. E. Fry, eds. Macmillan, New York.
12. Fontem, D. A., Berger, R. D., Weingartner, D. P., and Bartz, J. A. 1991. Progress and spread of dark leaf spot in cabbage. Plant Dis. 75:269-274.
13. Frantzen, J., and van den Bosch, F. 2000. Spread of organisms: Can travelling and dispersive waves be distinguished? Basic Appl. Ecol. 1:83-91.
14. Fried, P. M., MacKenzie, D. R., and Nelson, R. R. 1979. Dispersal gradients from a point source of *Erysiphe graminis* f. sp. *tritici* on Chancellor winter wheat and four multilines. Phytopathol. Z. 95:140-150.
15. Gregory, P. H. 1948. The multiple infection transformation. Ann. Appl. Biol. 35:412-417.
16. Gregory, P. H. 1968. Interpreting plant disease dispersal gradients. Annu. Rev. Phytopathol. 6:189-212.
17. Inman, A. J., Fitt, B. D. L., Todd, A. D., and Evans, R. L. 1999. Ascospores as primary inoculum for epidemics of white leaf spot (*Mycosphaerella capsellae*) in winter oilseed rape in the UK. Plant Pathol. 48:308-319.
18. Kiyosawa, S., and Shiyomi, M. 1972. A theoretical evaluation of mixing resistant variety with susceptible variety for controlling plant diseases. Ann. Phytopathol. Soc. Jpn. 38:41-51.
19. Lambert, D. H., Villareal, R. L., and Mackenzie, D. R. 1980. A general model for gradient analysis. Phytopathol. Z. 98:150-154.
20. Maffia, L. A., and Berger, R. D. 1999. Models of plant disease epidemics. II: Gradients of bean rust. J. Phytopathol. 147:199-206.
21. McCartney, H. A., and Bainbridge, A. 1984. Deposition gradients near to a point source in a barley crop. Phytopathol. Z. 109:219-236.
22. Minogue, K. P. 1986. Disease gradients and the spread of disease. Pages 285-310 in: Plant Disease Epidemiology, Vol. 1. K. J. Leonard and W. E. Fry, eds. Macmillan, New York.
23. Mollison, D. 1977. Spatial contact models for ecological and epidemic spread. J. R. Statist. Soc. B 39:283-326.
24. Mundt, C. C. 1989. Use of the modified Gregory model to describe primary disease gradients of wheat leaf rust produced from area sources of inoculum. Phytopathology 79:241-246.
25. Mundt, C. C., and Leonard, K. J. 1985. A modification of Gregory's model for describing plant disease gradients. Phytopathology 75:930-935.
26. Paysour, R. E., and Fry, W. E. 1983. Interplot interference: A model for planning field experiments with aerially disseminated pathogens. Phytopathology 73:1014-1020.
27. Sackett, K. E., and Mundt, C. C. 2005. The effects of dispersal gradient and pathogen life cycle components on epidemic velocity. Phytopathology 95:992-1000.
28. Shaw, M. W. 1995. Simulation of population expansion and spatial pattern when individual dispersal distributions do not decline exponentially with distance. Proc. R. Soc. Lond. B Biol. Sci. 259:243-248.
29. Shrum, R. 1975. Simulation of wheat stripe rust (*Puccinia striiformis* West.) using EPIDEMIC, a flexible plant disease simulator. Prog. Rep. Pap. Agric. Exp. Stn. 347.
30. Zadoks, J. C. 2001. Plant disease epidemiology in the twentieth century: A picture by means of selected controversies. Plant Dis. 85:808-815.
31. Zadoks, J. C., and Kampmeijer, P. 1977. The role of crop populations and their deployment, illustrated by means of a simulator, EPIMUL76. Ann. N.Y. Acad. Sci. 287:164-190.
32. Zwankhuizen, M. J., Govers, F., and Zadoks, J. D. 1998. Development of potato late blight epidemics: Disease foci, disease gradients, and infection sources. Phytopathology 88:754-763.